Benchmark analysis of in-vacuum vessel LOCA scenarios for code-to-code comparison

Benchmark analysis of in-vacuum vessel LOCA scenarios for code-to-code comparison

Matteo D'Onorio [(a)], Salvatore D'Amico [(b)], Antonio Froio [(c)], Maria Teresa Porfiri [(d)], Gandolfo Alessandro Spagnuolo [(e)], Gianfranco Caruso [(a)]

[a] *DIAEE, Sapienza University of Rome, Corso Vittorio Emanuele II, 244, 00186 Roma, Italy*
[b] *Karlsruhe Institute of Technology (KIT), Institute for Neutron Physics and Reactor Technology (INR), Hermann-von-Helmholtz-Platz 1, 76344 Eggenstein-Leopoldshafen, Germany*
[c] *NEMO group, Dipartimento Energia, Politecnico di Torino, Corso Duca degli Abruzzi, 24, 10129 Torino, Italy*
[d] *EUROfusion Consortium, Programme Management Unit, Garching, Germany*

Computer modeling codes represent a crucial tool to support the design of future fusion plants. Since one of the most important functions that codes must achieve is assessing safety systems design, a verification and validation phase is required. In this framework, a code-to-code comparison among four codes has been carried within EUROfusion consortium between Safety Analyses and Environment and Balance of Plant work packages.

In particular, an in-vessel Loss of Coolant Accident has been selected as a benchmark scenario for investigating thermal-hydraulic parameters of the vacuum vessel and its suppression system. This paper aims to compare the answer of different codes in terms of peak pressure within the vacuum vessel and its timing, the equilibrium pressure, and relief valve and rupture disk opening using a simplified thermal-hydraulic model of the EU-DEMO. In order to minimize the differences among the codes, the models have been kept to the simplest possible nodalization, successively increasing the model complexity.

Keywords: LOCA, Vacuum vessel, EU DEMO, Safety, Thermal-hydraulic benchmark

1. Introduction

The EU-DEMO reactor is planned to be the first European fusion reactor to produce net electricity from fusion. It has recently entered the conceptual design phase [1] and, for this reason, safety analyses are becoming essential for driving the design, as all the main plant subsystems must be designed to withstand Design-Basis Accidents (DBA) scenarios.

Computational safety analysis tools must be verified and validated to ensure that codes reflect reality with conservative safety margins. In the past years, several experimental activities on existing facilities, like the ICE facility at JAERI (Japan) [2] and the EVITA facility at CEA (France) [3], have been performed for validating computer codes or specific models developed for simulating fusion reactors behavior [4]. After these experimental campaigns, existing codes have undergone many improvements, and fusion-adapted versions have been released. Most of these codes have been used for supporting ITER licensing procedures [5] and for the safety demonstration of different Test Blanket Module (TBM) concepts [6][7]. However, because of the power scale-up and other design differences between ITER and DEMO plants, many of the accidental transients studied in ITER DEMO could have different consequences in DEMO, making the experience gained in past activities not directly applicable. For this reason, verification and validation activities are still needed.

In past years, a functional failure modes and effects analysis for all EU-DEMO key systems selected 21 postulated initiating events that envelope all identified failures [8]. Among these, in-vessel Loss Of Coolant Accident (LOCA) has been classified as one of the most representative events in challenging conditions for plant safety. For this reason, an in-vessel LOCA has been selected as a reference accident scenario for this activity, which aims to perform a code-to-code comparison among four different codes used within the EUROfusion Consortium and, more in general, within the scientific fusion community (e.g., CONSEN, GETTHEM, MELCOR, and RELAP5-3D).

In particular, the main objective of the work is to compare the answers of four selected codes, in terms of peak pressure within the Vacuum Vessel (VV), equilibrium pressure and their timing, as well as the timing of the Rupture Discs (RDs) opening, in conditions relevant for the EU-DEMO reactor.

2. Involved codes

The benchmark analysis is carried out with four system codes that have already been applied to EU-DEMO [9]-[16] and TBM [6][7] relevant safety analyses for both helium and water-cooled Breeding Blankets (BB). In addition, MELCOR and RELAP codes have also been applied to the Korean Helium Cooled Solid Breeder (HCSB) TBM [17] and the JA-DEMO reactor [18]. A short description of the involved codes and their application to the fusion-safety field is provided below.

author's email: matteo.donorio@uniroma1.it

- CONSEN (*CONServation of ENergy*) [19] is a fast-running code developed by the University of Rome "La Sapienza" and ENEA since 1990 to simulate thermal-hydraulics transients between the interconnected control volumes affected by accident, with particular reference to fusion reactor conditions. The code solves mass, momentum, and energy equations. It evaluates the thermodynamic evolution of fluids, including the change of phase and the treatment of thermodynamic conditions below the triple point of phase water. CONSEN has been included in the activities relating to code validation promoted inside the Euratom Fusion Technology Programme to test the capability of codes in simulating phenomena expected in case of accidents in fusion facilities and, specifically, in the ITER plant [20][21]. Particularly, CONSEN has been used in benchmark exercises of the codes in simulating thermo-hydraulic transients that occur during a loss of coolant accident inside a vacuum vessel and pre/post-test calculations for the ICE (Japan) [22] and EVITA (France) experimental campaigns [23]. A new version of the code, including liquid metals properties and phenomena, is under development.
- GETTHEM (*GEneral Tokamak THErmal-hydraulic Model*) [24] is a system-level code developed at Politecnico di Torino with EUROfusion support since 2015 for the thermal-hydraulic transient modeling for fusion power plants. The code aims to become a fully integrated code for the analysis of the different subsystems involved in the power generation in tokamak fusion reactors, including the BB, balance-of-plant, the tritium extraction and removal system plant electrical systems. It has been applied in the past for the analysis of normal operation [25][26] and accidental transients, including benchmark [27] and validation exercises. Its module for accidental analyses, developed from the open-source ThermoPower Modelica library [28], allows a fast evaluation of in-vessel and ex-vessel LOCAs. The code can be used with different working fluids, including water, helium, air, and lithium-lead.
- MELCOR [29] is a fully integrated severe accident code based on a control volume approach. It can simulate the thermal-hydraulic phenomena in steady and transient conditions and the main severe accident phenomena characterizing the progression of accident sequences. The fusion safety group of Idaho National Laboratory (INL) has recently modified MELCOR for fusion applications [30]. The fusion version of the MELCOR code (ver. 1.8.6) simulates coolant thermal-hydraulic behavior and radionuclide and aerosol transport in nuclear facilities and reactor cooling systems during severe accident scenarios. MELCOR can also predict structural temperatures (e.g., First Wall (FW), blanket, divertor, and vacuum vessel) resulting from energy produced by radioactive decay heat and oxidation reactions. MELCOR 1.8.6 for fusion underwent a standard benchmarking exercise before its release [31]. Two sub-versions of the MELCOR code are available: a DBA version, which includes conservativism for material oxidation and aerosol deposition mechanisms, and a beyond design basis accident version which has no conservativisms and is promoted as a best estimate calculation tool. For this work, the DBA version has been used.
- RELAP5-3D (*Reactor Excursion and Leak Analysis Program*) [32] is a fully integrated, multi-dimensional thermal-hydraulic developed at INL to analyze transients and accidents in water-cooled nuclear power plants and related systems as well as the analysis of advanced reactor designs. The code can be used for systems applying the DEMO relevant working fluids water, helium, hydrogen, lithium, lithium-lead, molten salts, or nitrogen. RELAP5-3D has been validated for fusion applications. Code validation with experiments of the HELOKA-HP facility at KIT/INR has been done by means of the heater model for the first step. With the BEST-EST module, the model parameters have been calibrated as well. The validation and calibration procedure has been published in [33].

3. Reference cases modelling

In order to compare the four codes, the simplest possible model has been chosen; a schematic view of the thermal-hydraulic model is reported in Figure 1.

The reference accident sequence is the "baseline" scenario described in [34]. The in-vessel LOCA is caused by a double-ended guillotine rupture of the breeding zone's largest feeding pipe in the upper port. The corresponding flow area is reported in Figure 1. Considering that limiters could be introduced in the future design of DEMO to prevent damages to plasma-facing components, it has been assumed that energy deposited by an unmitigated plasma shutdown is successfully absorbed by limiters, preventing the failure of the first wall structure. Both BB Concepts, namely the Helium-Cooled Pebble Bed (HCPB) and a Water-Cooled Lithium Lead (WCLL), are analyzed.

For the sake of simplicity, no actively-operated bleed valves are included in the models, as they are not expected to play a significant role in the case of a large-break LOCA like the one considered here.

The benchmark is carried out in two steps: in the first one, only hydraulic components ("control volumes") are included in the model (i.e., with no Heat Structures (HS) masses). In the second step, HS are included in the model to analyze the effect of the metallic mass of the Vacuum Vessel, Relief Lines (RL), and Expansion Volumes (EV). The design data for the RL heat structure have been taken from the CAD model in [35] to simulate the stainless steel mass of the pipework connecting the VV upper port to the VV Pressure Suppression System (VVPSS) tanks. The structure surrounding the VV volume is modeled to represent the torus-shaped double-walled vacuum vessel of EU-DEMO. This heat structure is modeled in a cylindrical approximation; the thickness has been

modified, maintaining the total mass of the austenitic stainless steel of the VV main body, in order to preserve the characteristic time scales of the heat transfer phenomena.

The expansion volumes have been used to model the function of the VVPPS tanks. The VV pressure suppression system is one of the most critical safety systems to be foreseen in the EU-DEMO plant since it confines the radioactive sources term and limits the VV peak pressure in the event of in-vessel LOCA. The VVPSS consists of 6 different expansion tanks. One of them is dry and is used to handle small leakages. The other tanks are filled with water and have a suppression function. A detailed description of the system is reported in [34]. In the current analysis, the wet suppression tanks have been modeled with a single control volume. In particular, for the water case, two possible configurations of the EV are investigated: one featuring a dry EV only (Case I); and one including also a wet EV (Case II). For the helium case, only the presence of a dry EV has been considered (Case I). In addition, two different nodalization schemes for the VV have been adopted for both helium and water: a single volume (in Case I and Case II) and a more refined nodalization according to Figure 2b (in Case III). In this latter case, as shown in Figure 2a, five different control volumes have been used to represent different VV compartments: Upper Port (UP), Plasma Chamber (PC), Lateral VV (i.e., the space between the back of the breeding blanket and the VV wall), bottom divertor (i.e., the free space below the divertor) and Lower Port. Case III aims to evaluate the effects of a different nodalization on relevant quantities such as peak pressure and timing.

The detail of the parameters of the different cases is reported in Table 1. At the initial condition, the volume representing the PHTS+BB is filled with either helium or water, according to the corresponding BB variant (i.e., HCPB or WCLL). In contrast, all the other volumes are assumed to be filled with air. In principle, the VV should be filled with a mixture of hydrogen and helium; however, the small mass contained therein is not expected to have any relevant impact on the results.

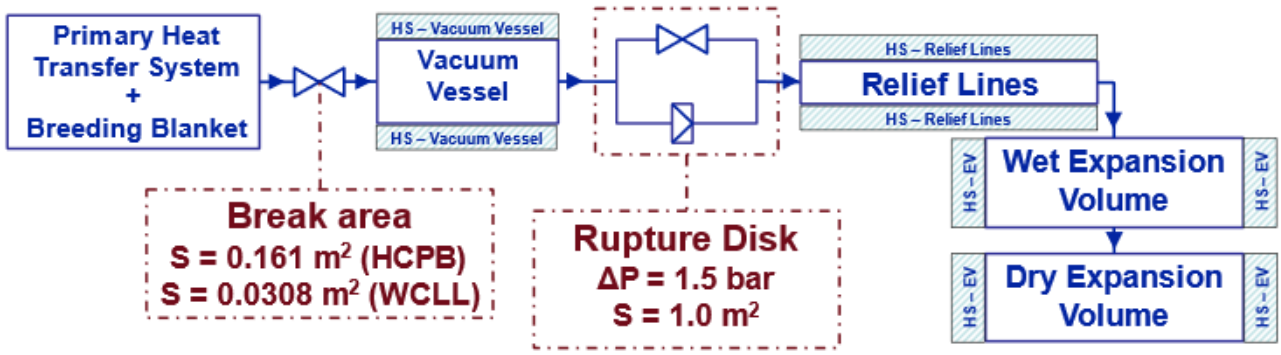

Figure 1. Schematic view of the adopted model

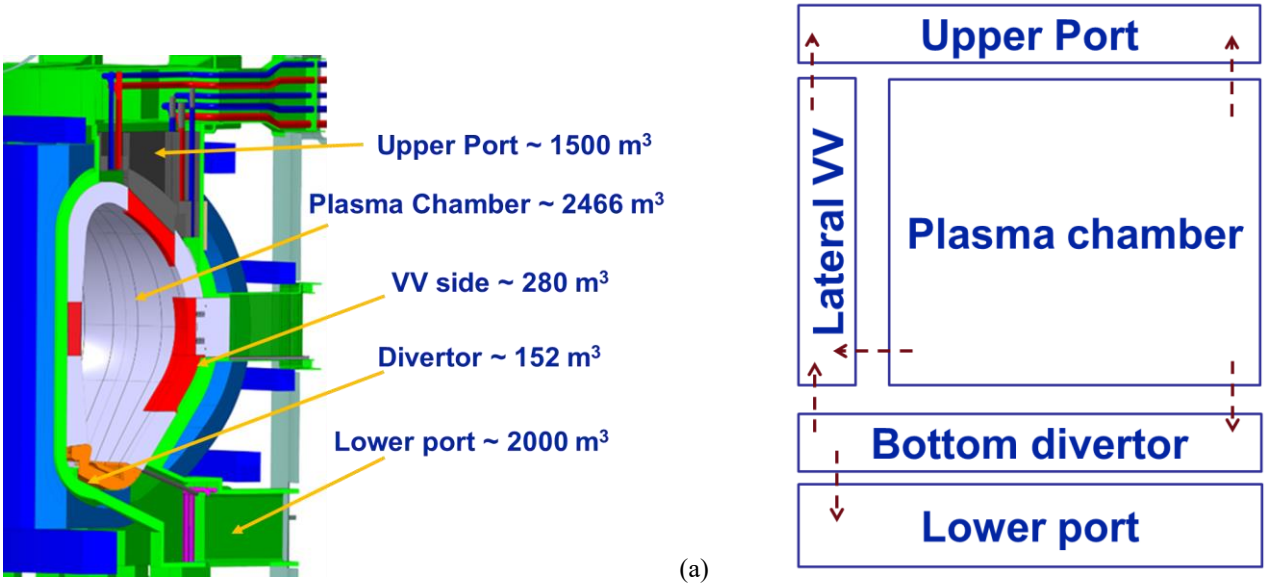

Figure 2. (a) identification of the five different volumes included in the VV; (b) nodalization used for the VV in Case III.

Table 1. Initial conditions and volumes.

		Pressure [bar]		Temperature [K]		Volume [m³]	
		WCLL	HCPB	WCLL	HCPB	WCLL	HCPB
Case I to III	PHTS + BB	155	80	568.65	683.15	326.0	215.5
Case I to III	VV	10^{-5}		573.15		6400	
Case I to III	RL	0.95		293.15	313.15	48×5	48×3
Case II & III WCLL	WET EV	0.95		293.15	313.15	500×5 (60% H_2O)	-
Case I to III	DRY EV	0.95		293.15	313.15	500×5	1000×3

Table 2. Heat Structures data.

	R_i [m]	**R_e [m]**	**H [m]**	**Initial T [K]**	**BC type @Si**	**BC type@Se**
VV	13	13.6	20.5	573.15	HTC = 15 [W/Km²]	Adiabatic
RL	0.564	0.569	24.5	313.15 (WCLL)	HTC = 150 [W/Km²]	Adiabatic
				293.15 (HCPB)		
EV	4.795	4.8	6	313.15 (WCLL)	HTC = 15 [W/Km²]	Adiabatic
				293.15 (HCPB)		

Concerning the HS, the metallic masses of the VV, RL, and EV (both wet and dry, where applicable) are considered. Also in this case, the simplest possible model has been chosen, modeling masses with the shape of a hollow cylinder. A single volume in the axial direction is adopted for all HSs, discretized with 11 nodes (boundaries included) in the radial direction. For all the heat structures, an adiabatic Boundary Condition (BC) has been imposed on the outer surface, while a convective BC has been set on the inner surface. In particular, to minimize the modeling differences among the four codes, a fixed Heat Transfer Coefficient (HTC) has been used. The parameters of the HS used in this work are reported in Table 2; the initial condition is taken uniformly equal to the temperature of the associated fluid control volume.

4. Results of benchmark activity

In the following, the four codes are compared in terms of the most relevant thermal-hydraulic results, at first for the models without heat structures and then for the models including heat structures. A 600 s transient after the postulated initiating event is simulated. The accident transient starts at $t = 0.0$ s, assuming an opening between the "PHTS + BB" volume and the VV volume.

4.1. Without heat structures

4.1.1 Main results for HCPB cases

As concerns the first step of the benchmark, the starting point has been assessing the HCPB scenarios. In particular, two different scenarios have been envisaged for this concept which differs only for the VV modeling approach, as reported in Table 1. The primary purpose has been the evaluation of pressure and temperature behaviors, determining if there are any deviations when considering the hydraulic resistances among the VV main sub-divisions (see Figure 2b).

After the break, helium flows from the PHTS volume to the VV through the break junction. The maximum mass flow rate is up to 800 kg/s for all the system codes, and it is predicted soon after the break opening. The total mass of helium entering the VV is reported in Table 3. The injection of helium inside the VV causes rapid pressurization of the volume. Figure 3 shows the pressure waveform in the "PHTS + BB" volume, highlighting the excellent agreement between the four codes in predicting the blowdown phase of the control volume. Pressure decreases from 80 bar to around 1.9 bar in around 6s, when the mechanical equilibrium with the VV volume is reached. Pressure in VV volume is shown in Figure 4. Despite small differences in the pressure increasing trend, the equilibrium values are in good agreement among the four codes, with values ranging between 0.1927 MPa and 0.1983 MPa (max variation ~2.9 %). The pressure increase in the VV is mitigated by the opening of rupture discs, connecting the VV to suitable expansion volumes. The triggering occurs when differential pressure between the VV and the BL volume is higher than 150 kPa. In Table 3, the time at which the triggering occurs is reported.

In Figure 5 and Figure 6, the temperature waveforms are reported for the VV and the EV volumes, respectively.

A minor mismatch, with a maximum deviation of about 4%, can be observed in evaluating the temperatures in the two volumes.

Concerning HCPB Case III, results related to plasma chamber pressure and Mass Flow Rate (MFR) toward rupture disks are shown in Figure 7 and Figure 8, respectively. All the codes well predict pressure increase in PC volume. Pressure raises from 1 Pa to around 1.9 bar in 5.9 s. Rupture discs' triggering is well predicted by the four different codes, with opening time ranging between 0.78 s and 0.87 s. As soon as the RDs open, a spike in the injected MFR occurs with values ranging between 140 kg/s and 160 g/s. MFR decreases to zero in around 6 s. It should be noted how the more detailed nodalization of the VV volume affects the accident transient, with faster pressurization of the upper port volume and an earlier triggering of the RDs.

As can be derived from Table 3, the four involved codes are in relatively good agreement in evaluating the main parameters in both the two HCPB scenarios, which practically show the same pressure evolution inside the VV. The slight variations observed in the equilibrium values are mainly due to the different helium inventory discharged to the VV.

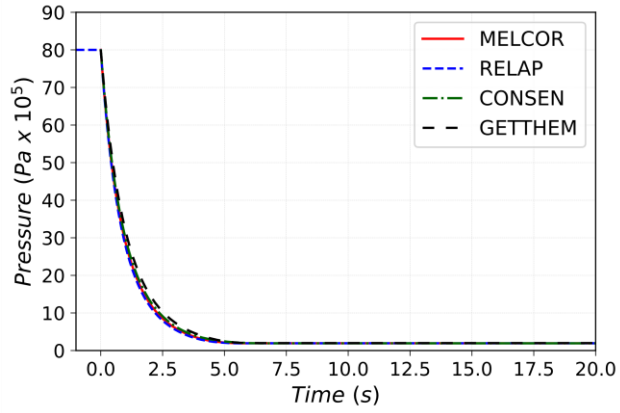

Figure 3. HCPB Case I: Pressure in PHTS+BB volume

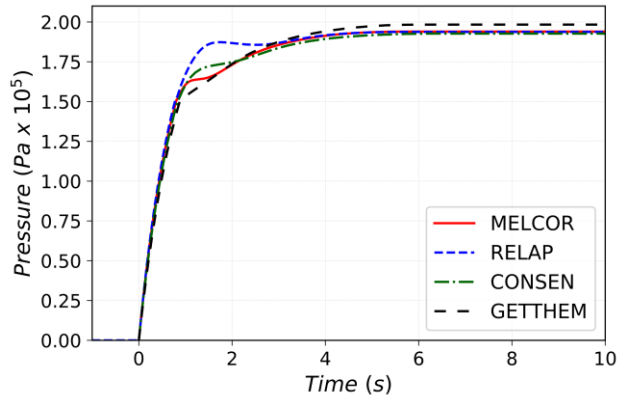

Figure 4. HCPB Case I: Pressure in VV volume

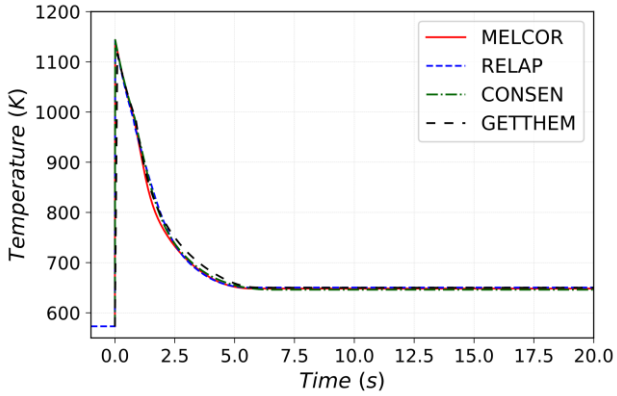

Figure 5. HCPB Case I: VV temperature

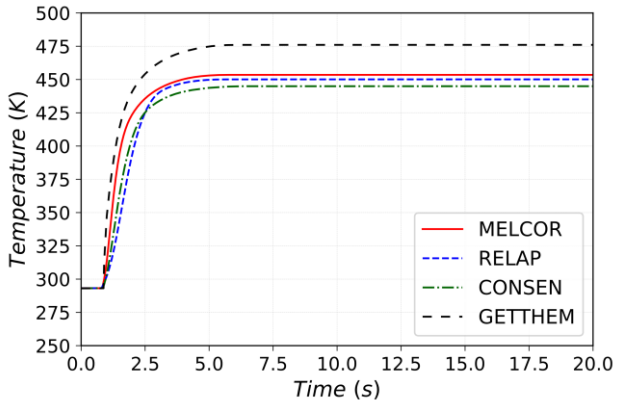

Figure 6. HCPB Case I: Temperature in EV

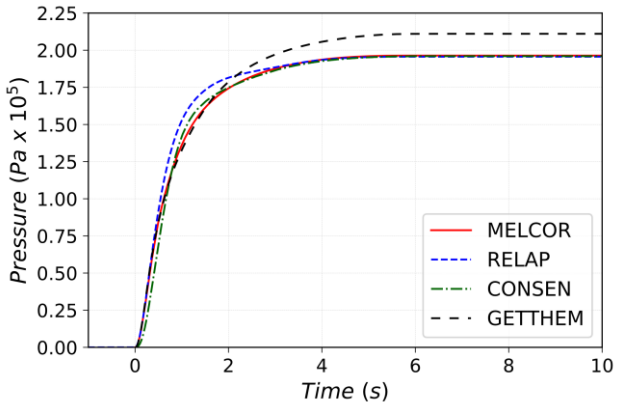

Figure 7. HCPB Case III: Pressure in PC volume

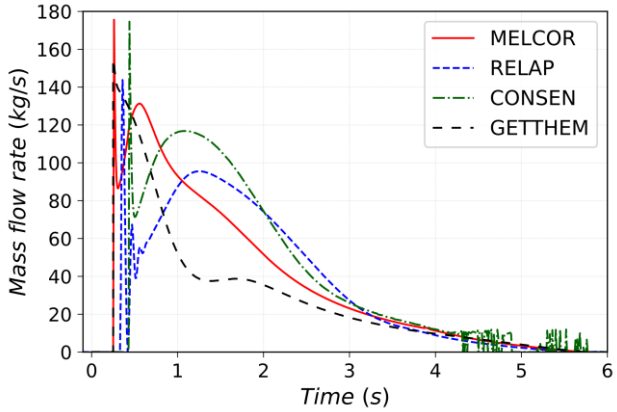

Figure 8. HCPB Case III: Mass Flow Rate in Relief Lines

Table 3. Summary results for HCPB Cases. (NB: CONSEN results are taken as the reference; the columns for the other codes report the percentage relative difference with respect to CONSEN.)

	Case I				Case III			
	CONSEN	MELCOR	RELAP	GETTHEM	CONSEN	MELCOR	RELAP	GETTHEM
p_{max} VV [MPa]	0.1927	0.6227 %	0.5189 %	2.906 %	0.196	0.1531 %	-0.2041 %	7.653 %
T_{eq} VV [K]	646.1	0.3483 %	0.6640 %	0.6191 %	1656	-50.09 %	-74.90 %	-57.06 %
T_{max} VV [K]	1144	-0.008744 %	-0.04372 %	-2.387 %	2580	2.472 %	-55.93 %	-55.99 %
Break Integral MFR [kg]	1067	0.6065 %	-0.1997 %	4.806 %	1066	0.5321 %	-0.1408 %	1.480 %
RDs opening time [s]	0.84	-3.6 %	-7.1 %	3.6 %	0.44	-41 %	-23 %	-43 %
Integral RDs MFR [kg]	150.5	-1.927 %	-0.4917 %	-0.4385 %	231.4	-6.758 %	-12.08 %	-28.94 %

4.1.2 Main results for WCLL cases

For the WCLL, all three cases reported in Table 1 have been studied. The transient evolution is qualitatively similar to that obtained for the HCPB case but with much longer timescales and a peak mass flow rate of ~3000 kg/s. In Case I, the absence of the wet EV strongly reduces the pressure suppression, yielding a substantial pressure buildup in the VV higher than 1.5 MPa, with an evolution similar to that found in the case with HS (reported below in Figure 16). The four codes predict similar thermal-hydraulic behavior, with a discrepancy in the equilibrium temperature in the EV (see Figure 9). However, it should be noted that the relevance of this case for the EU-DEMO is limited, as a pressure as high as 1.5 MPa would not be withstandable by the VV, and a wet EV is necessary. Conversely, in Case II, because of steam suppression in the wet tank, the pressure in the VV stabilizes immediately after RD triggering, which is captured with reasonable accuracy by all four codes, as visible in Figure 10. The main outcomes of Case II and Case III are reported in Table 4. The most relevant quantitative difference among the four codes is the total mass discharged to the EVs ("Integral RDs MFR" in Table 4), which for GETTHEM is very close to the total mass discharged from the PHTS. The reason for this behavior is that a fully homogeneous (equilibrium) model is implemented in GETTHEM, so that, after the RDs are triggered, both liquid and vapor are discharged from the VV, and a larger mass flow rate is computed as opposed to the other three codes. This assumption is planned to be relieved in future releases of the code [12].

For WCLL Case III, Figure 11 and Figure 12 report the mass flow rate at the break junction and the pressure in the plasma chamber volume, respectively.

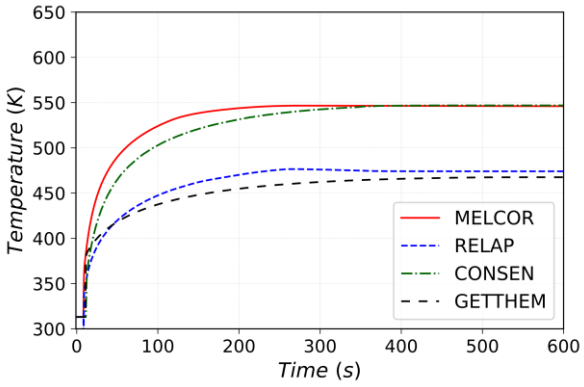

Figure 9. WCLL Case I: Temperature in EV

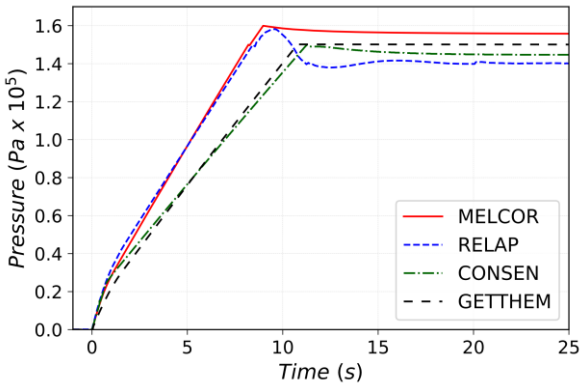

Figure 10. WCLL Case II: VV volume pressurization

Table 4. Summary results for WCLL Case II and III. (NB: CONSEN results are taken as reference; the columns for the other codes report the percentage relative difference with respect to CONSEN.)

	Case II				Case III			
	CONSEN	MELCOR	RELAP	GETTHEM	CONSEN	MELCOR	RELAP	GETTHEM
p_{max} VV [MPa]	0.1501	5.929 %	5.263 %	-0.06662 %	0.151	3.311 %	5.96 %	-0.6623 %
p_{eq} VV [MPa]	0.1501	3.931 %	-9.394 %	-6.063 %	0.151	2.649 %	3.974 %	-7.947 %
T_{eq} VV [K]	384.5	0.3100 %	-0.7406 %	-0.4806 %	384.7	15.92 %	1.391 %	12.03 %
T_{max} VV [K]	573.15	0 %	0 %	0 %	573.15	0 %	2.971 %	0 %
Integral break MFR [kg]	227000	-14.98 %	0.4405 %	0 %	228000	-15.35 %	-3.947 %	0.8772 %
RDs opening time [s]	11.24	-27.95 %	-25.01 %	-4.199 %	10.3	-37.57 %	-15.92 %	7.01 %
Integral RDs MFR [kg]	88210	-0.5246 %	3.23 %	142.9 %	88790	-1.306 %	-4.52 %	143.6 %

All the four codes predict the same mass flow rate evolution, except MELCOR due to different handling of the fluid phase in the upstream volume (which is split in pool and atmosphere for MELCOR, and is homogeneous for the other three). Nevertheless, the total mass discharged (i.e., the integral of the curve in Figure 11) is similar for all four codes, as reported in Table 4. Concerning the PC pressure, the codes predict a qualitatively similar behavior, with differences mainly identifiable with the different choke models used by the different codes.

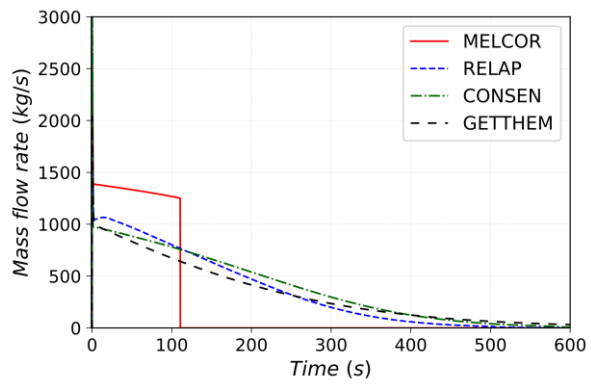

Figure 11. WCLL Case III: Mass Flow Rate from break

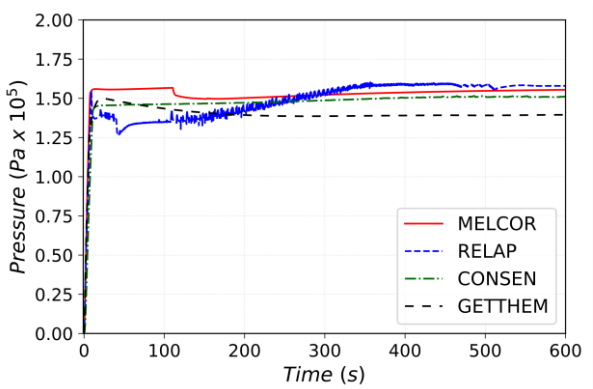

Figure 12. WCLL Case III: Pressure in PC volume

4.2. Results with heat structures

4.2.1 Main results for HCPB case I

Concerning the results with heat structures, Case III has been excluded from the analysis, as it has been shown that the detailed nodalization does not significantly affect the results. Hence, only Case I has been studied for HCPB and Case I and Case II for WCLL.

In Figure 13, the VV pressurization waveform is shown for HCPB Case I. The trend is very similar to the one described in Figure 3 for the case without structures. After the junction opening simulating the pipe break, coolant starts to flow from the PHTS and BB volume into the VV one with a maximum mass flow rate ranging between 730 and 820 kg/s depending on the code. The helium injection inside the VV leads to fast pressurization of the VV volume, which is well predicted by the four codes. Slight differences in the pressurization trend start at the opening of the relief lines, ranging between 0.78 s and 0.88 s.

However, such differences do not affect the equilibrium pressure value equal to 1.89 bar for RELAP, MELCOR and CONSEN, while GETTHEM predicts a slightly higher pressure value of 1.96 bar.

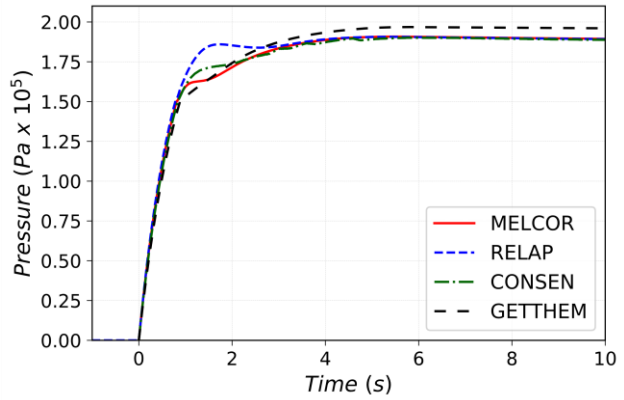

Figure 13. HCPB Case I: Pressure in VV

As specified in Table 2, the VV has been modeled as a cylindrical mass of 7.157×10^6 kg of SS. Because of this huge mass, the temperature of the VV heat structure remains constant and equal to the initial value of 573.15 K in all the HS nodes for the entire simulation. An internal heat structure surface of 1674.0 m² with an HTC equal to 15 W/(m² K) allows heat transfer from the structure to the VV control volume. At the end of the simulation, the gas temperature in the VV control volume is slightly lower (around 572.0 K) than the temperature of the associated heat structure. All the involved codes well predict this phenomenon.

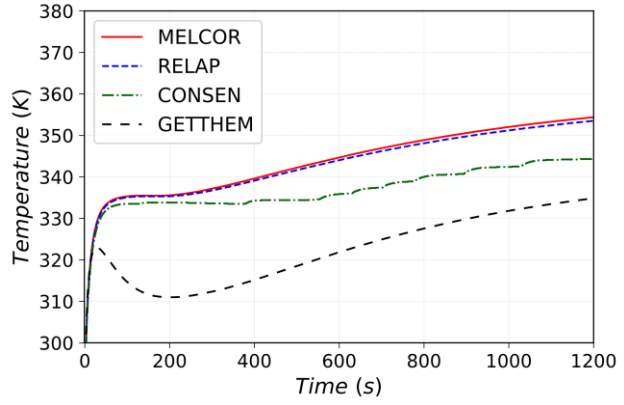

Figure 14. HCPB Case I: Temperature of RL HS

In Figure 14, the temperature at the intermediate node of the RL heat structure is shown. As specified in Table 2, the RL HS has been modeled as a cylindrical mass of 3458.0 kg of SS, 5 mm thick, and an internal heat transfer surface of 86.82 m². A heat transfer coefficient of 150 W/(m² K) has been assumed to simulate heat transfer with the corresponding volume. Concerning the temperature waveform GETTHEM underestimates the initial temperature increase, as most of the heat is advected by the helium in the RL rather than transferred by convection to the corresponding HS. This is proven by the larger temperature increase predicted by the same code in the downstream EV HS, which acts as the final heat sink, as reported in Figure 15. At the end of the simulation CONSEN, GETTHEM, and MELCOR predict a temperature in the RL HS around 345 K, whereas in RELAP the central node of the HS reaches a temperature above 370 K. This is due to the higher temperature of the helium flowing inside the RL control volume. Main results of the HCPB simulation are reported in Table 5.

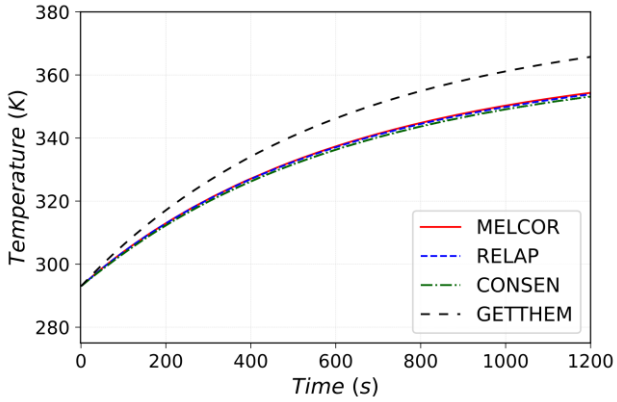

Figure 15. HCPB Case I: Temperature of EV HS

4.2.2 Results for WCLL cases

Figure 16 reports the pressure evolution in the VV volume for the WCLL Case I. As anticipated for the case without HS, the absence of the wet EV causes a large pressure (15 bar) to be reached, which is well predicted by all the codes; the main exception is RELAP which conservatively foresees a larger pressure buildup. This phenomenon happens because in the RELAP simulation all the water in the PHTS vaporizes because of its depressurization, causing a higher VV pressurization. This effect is also visible in the temperature evolution in the downstream volume (RL) and its associated HS, which is reported in Figure 17: indeed, the larger enthalpy content associated with fully-vaporized water in the VV is converted into a larger temperature increase in the RL HS, with RELAP computing an equilibrium temperature therein of 511 K, as opposed to the 473 K predicted by the other three codes (see Table 6).

Concerning the other HSs, the temperature in the central node of the EV HS is shown in Figure 18. In this case, MELCOR and CONSEN predict a faster temperature increase with respect to RELAP and GETTHEM; detailed results are reported in Table 6. The VV HS temperature is basically constant for the same reason highlighted above for the HCPB case. Note that, also in this case, the relevance of this scenario to the EU-DEMO is questionable due to the absence of the wet EV, and it is reported here only for the sake of the code-to-code comparison.

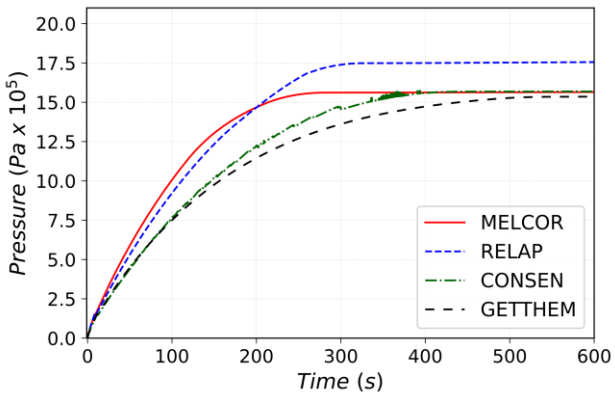

Figure 16. WCLL Case I: Pressure in VV volume

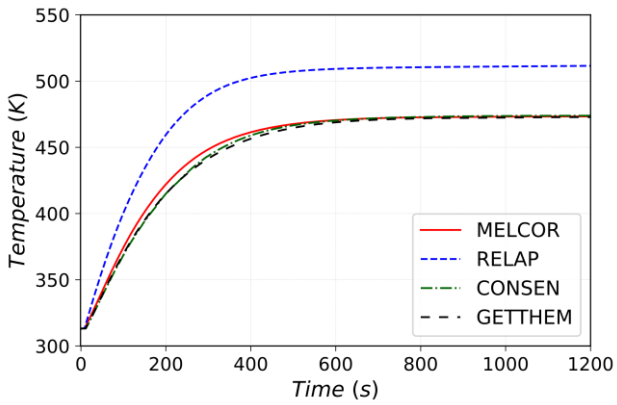

Figure 17. WCLL CASE I: Temperature of RL HS

Table 5. HCPB Case I main results with heat structures. (NB: CONSEN results are taken as reference; the columns for the other codes report the percentage relative difference with respect to CONSEN.)

	CONSEN	MELCOR	RELAP	GETTHEM
p_{max} VV [MPa]	0.19	0 %	0 %	3.158 %
p_{eq} VV [MPa]	0.168	-1.19 %	-1.19 %	2.976 %
T_{eq} VV [K]	572.6	-0.04715 %	0.09605 %	-0.05589 %
T_{max} VV [K]	1140	-0.1930 %	-0.2719 %	-0.9298 %
Integral break MFR [kg]	1080	-0.5202 %	-0.3953 %	0.5258 %
RDs opening time [s]	0.85	-3.529 %	-8.235 %	4.706 %
Integral RDs MFR [kg]	176.5	-0.01133 %	0.6631 %	-9.861 %
T_{end} VV struct. [K]	573.15	0.001745 %	0 %	0.003489 %
T_{end} RL struct. [K]	344.5	4.029 %	3.141 %	-2.804 %
T_{end} EV struct. [K]	351.1	2.073 %	1.632 %	4.17 %

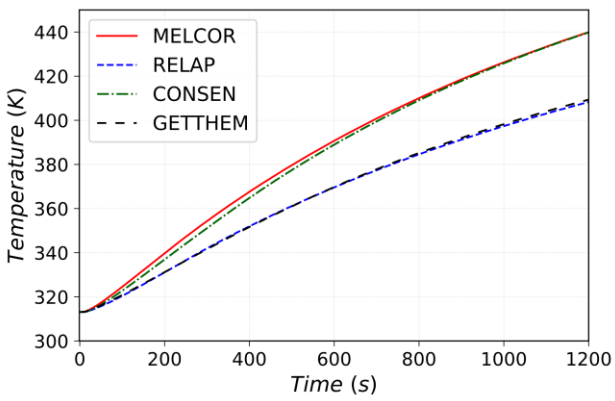

Figure 18. WCLL Case I: Temperature of EV HS

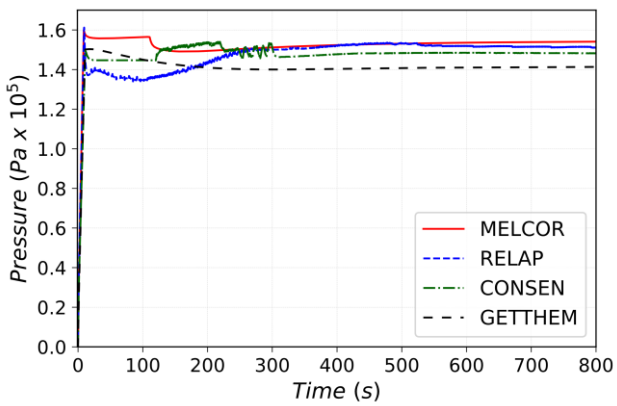

Figure 19. WCLL Case II: Pressure in VV volume

The pressure evolution in the VV for WCLL Case II is reported in Figure 19. It is clear that all the four codes predict similar behavior, with the same qualitative differences already commented for the case without heat structures. For the HS, MELCOR, RELAP, and CONSEN predict the same temperature evolution in the RL HS; indeed, GETTHEM predicts most of the energy in the fluid to be released to wet EV HS, as visible in Figure 21, overestimating the temperature increase therein and underestimating that in the other two HSs (RL and dry EV) with respect to the other codes (as reported in Figure 20 and Figure 22, respectively). However, this difference is almost fully recovered before the transient end, when the temperature predicted by GETTHEM in the three volumes is similar to that predicted by the other three codes, see Table 6.

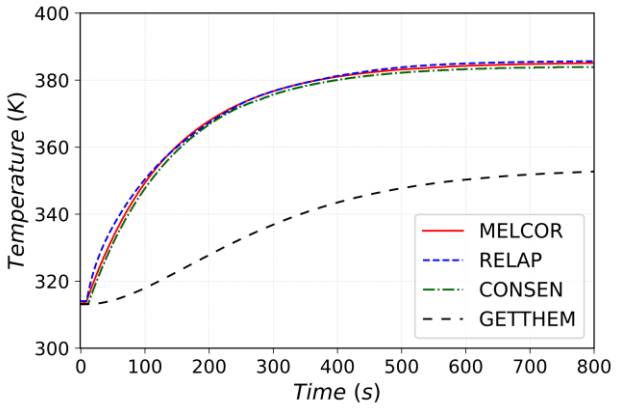

Figure 20. WCLL Case II: Temperature of RL HS

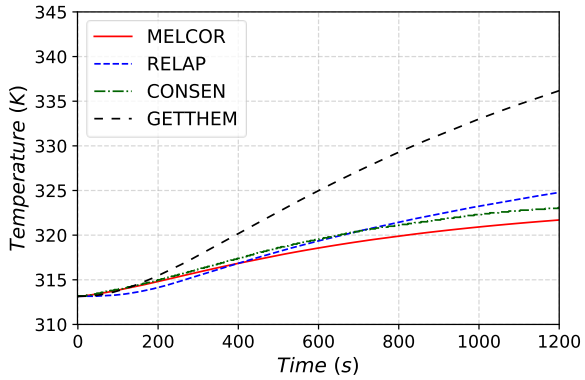

Figure 21. WCLL Case II: Temperature of Wet EV HS

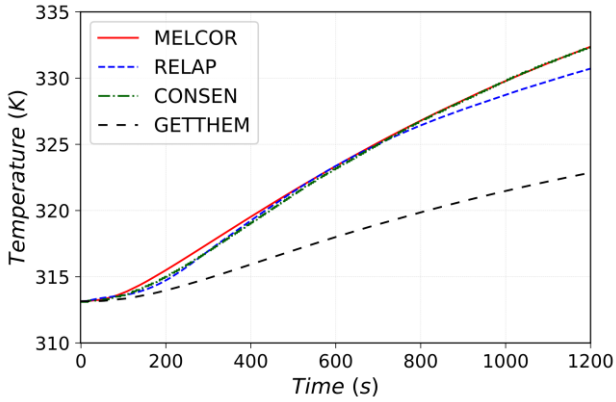

Figure 22. WCLL Case II: Temperature of Dry EV HS

Table 6. WCLL with heat structures main results. (NB: CONSEN results are taken as reference; the columns for the other codes report the percentage relative difference with respect to CONSEN.)

	WCLL Case I				WCLL Case II			
	CONSEN	MELCOR	RELAP	GETTHEM	CONSEN	MELCOR	RELAP	GETTHEM
p_{max} VV [MPa]	1.574	-0.03177 %	12.58 %	-1.639 %	0.154	3.247 %	-24.61 %	-2.597 %
p_{eq} VV [MPa]	1.574	0.03177 %	12.58 %	-1.639 %	0.148	4.054 %	2.027 %	-4.73 %
T_{eq} VV [K]	573.15	0 %	0 %	0 %	573.15	0 %	0 %	0 %
T_{max} VV [K]	473.7	0.02069 %	11.45 %	-0.163 %	384.1	0.3515 %	0.1796 %	-0.3541 %
Integral break MFR [kg]	218400	-33.38 %	-20.19 %	0.05403 %	227800	-20.11 %	-8.308 %	-0.003551 %
RDs opening time [s]	11.19	-26.99 %	-26.99 %	-4.379 %	11.19	-26.99 %	-21.45 %	-4.200 %
Integral RDs MFR [kg]	17110	2.572 %	16.41 %	236.2 %	91350	-0.8906 %	-2.449 %	137.8 %

T_{end} VV struct. [K]	573.15	-0.02268 %	-0.07327 %	-0.04013 %	573.15	-0.0314 %	-0.2634 %	-0.05757 %
T_{end} RL struct. [K]	473.9	-0.1224 %	7.945 %	-0.2258 %	384	0.3724 %	0.4818 %	-7.852 %
T_{end} dry EV struct. [K]	439.8	0.03411 %	-7.16 %	-6.921 %	332.4	-0.009025 %	0 %	-2.873 %
T_{end} wet EV struct. [K]	-	-	-	-	323.1	-0.4364 %	6.828 %	4.045 %

5 Conclusions and perspectives

A set of in-vessel LOCA scenarios, relevant for the EU-DEMO tokamak fusion reactor, has been used as a preliminary benchmark exercise for four codes used among the EUROfusion activities to compare the responses of the codes in several conditions. Both the loss of coolant from a helium-cooled and a water-cooled BB have been considered. Two cases have been selected for the helium scenario, whereas three cases have been used for the water scenario.

All the models developed with the four codes shared the same nodalization and modeling assumptions to minimize the differences whenever possible.

Initially, the outputs of the codes have been compared only from the hydraulic point of view, i.e., neglecting the presence of the metallic masses, with all the models predicting similar results in terms of pressure levels and timing. In addition, a model with a more articulate nodalization of the VV has been set up with all the codes, showing negligible differences with respect to the model with a single volume for the VV.

In the second phase, heat structures were added to the modeling to assess their thermal-hydraulics effects on the outcome. A fixed value of the HTC has been used to minimize the differences among the codes. Also in this case, the codes showed similar results, with however some differences to be ascribed to different models used in the codes (e.g., different models for choked flow).

While being outside of its aim, the work has also proved that, in all the considered scenario, the pressure in the VV does not overcome its limit of 2 bar, notwithstanding WCLL Case I where a wet EV was not considered.

In perspective, the benchmark exercise among the four codes shall be extended, adding step-by-step new layers of complexity in the models, e.g., including a heat exchanger in the EV, adding the Bleed Lines, or computing the HTC with known correlations. This work will continue during the Concept Design Phase of DEMO, identifying the potentialities as well as the limiting factors for each code. The final scope is the determination of each computational code's application field (e.g. design or safety analyses).

6 Acknowledgments

This work has been carried out within the framework of the EUROfusion Consortium and has received funding from the Euratom research and training programme 2014-2018 and 2019-2020 under grant agreement No 633053. The views and opinions expressed herein do not necessarily reflect those of the European Commission. A EUROfusion Engineering Grant financially supported the work of MDO, SDA, and AF.

7 List of abbreviations

BB	Breeding Blankets
BC	Boundary Conditions
DBA	Design-Basis Accidents
EV	Expansion Volume
FW	First Wall
HCPB	Helium-Cooled Pebble Bed
HCSB	Helium Cooled Solid Breeder
HS	Heat Structure
HTC	Heat Transfer Coefficient
LOCA	Loss Of Coolant Accident
MFR	Mass Flow Rate
PC	Plasma Chamber
RD	Rupture Discs
RL	Relief Line

TBM	Test Blanket Module
UP	Upper Port
VV	Vacuum Vessel
VVPSS	Vacuum Vessel Pressure Suppression System
WCLL	Water-Cooled Lithium Lead

8 References

[1] A. J. H. Donné, W. Morris, X. Litaudon, C. Hidalgo, D. McDonald, H. Zohm, E. Diegele, A. Möslang, K. Nordlund, G. Federici et al., European research roadmap to the realisation of fusion energy, EUROfusion Consortium, ISBN 978-3-00-061152-0, 2018.

[2] T. Kunugi, K. Takase, M. Shibata, R. Kurihara, Y. Seki, Thermofluid experiments on ingress of coolant event, Fusion Eng. Des., 42 (1–4) (1998), pp. 67-72, 10.1016/S0920-3796(98)00182-3

[3] P. Sardain, L. Ayrault, G. Laffont, F. Challet, L. B. Marie, B. Merrill, M. T. Porfiri, G. Caruso, The EVITA programme: experimental and numerical simulation of a fluid ingress in the cryostat of a water-cooled fusion reactor, Fusion Eng. Des., 75–79 (SUPPL.) (2005), pp. 1265-1269, 10.1016/j.fusengdes.2005.06.279

[4] L.N. Topilski, X. Masson, M.T. Porfiri, T. Pinna, L.-L. Sponton, J. Andersen, K. Takase, R. Kurihara, P. Sardain, C. Girard, Validation and benchmarking in support of ITER-FEAT safety analysis, Fusion Eng. Des., Volume 54 (3–4), 2001, pp. 627-633, 10.1016/S0920-3796(00)00575-5.

[5] N. Taylor, P. Cortes, Lessons learnt from ITER safety & licensing for DEMO and future nuclear fusion facilities, Fusion Eng. Des., 89 (2014), pp. 1995-2000, 10.1016/j.fusengdes.2013.12.030

[6] M. D'Onorio, D.N. Dongiovanni, I. Ricapito, J. Vallory, M.T. Porfiri, T. Pinna, G. Caruso, Supporting analysis for WCLL test blanket system safety, Fusion Eng. Des., 173, 2021, 112902, 10.1016/j.fusengdes.2021.112902.

[7] D. Panayotov, et al. Status of the EU test blanket systems safety studies, Fusion Eng. Des., 98-99 (2015), pp. 2201-2205, 10.1016/j.fusengdes.2014.12.016

[8] T. Pinna, D. Carloni, A. Carpignano, S. Ciattaglia, J. Johnston, M. T. Porfiri, L. Savoldi, N. Taylor, G. Sobrero, A. C. Uggenti et al. Identification of accident sequences for the DEMO plant, Fusion Eng. Des., 124 (2017) 1277-1280 10.1016/j.fusengdes.2017.02.026.

[9] G. Caruso and M. Nobili, Preliminary evaluation of the expansion system size for a pressurized gas loop: application to a fusion reactor based on a helium-cooled blanket, Int. J. Heat Technol. 35 (1) (2017) 211-218 10.18280/ijht.350128.

[10] G. Caruso and F. Giannetti, Sizing of the Vacuum Vessel Pressure Suppression System of a Fusion Reactor Based on a Water-Cooled Blanket, for the Purpose of the Preconceptual Design, Sci. Technol. Nucl. Install. (2016) 8719695 10.1155/2016/8719695.

[11] A. Froio, L. Barucca, S. Ciattaglia, F. Cismondi, L. Savoldi and R. Zanino, Analysis of the Effects of Primary Heat Transfer System Isolation Valves in case of In-Vessel Loss-Of-Coolant Accidents in the EU DEMO, Fusion Eng. Des. 159 (2020) 111926 10.1016/j.fusengdes.2020.111926.

[12] A. Froio, A. Bertinetti, S. Ciattaglia, F. Cismondi, L. Savoldi and R. Zanino, Modelling an In-Vessel Loss of Coolant Accident in the EU DEMO WCLL Breeding Blanket with the GETTHEM Code, Fusion Eng. Des. 136 (B) (2018) 1226-1230 10.1016/j.fusengdes.2018.04.106.

[13] M. D'Onorio, F. Giannetti, M. T. Porfiri and G. Caruso, Preliminary safety analysis of an in-vessel LOCA for the EU-DEMO WCLL blanket concept, Fusion Eng. Des. 155 (2020) 111560 10.1016/j.fusengdes.2020.111560.

[14] M. D'Onorio F. Giannetti, M. T. Porfiri and G. Caruso, Preliminary sensitivity analysis for an ex-vessel LOCA without plasma shutdown for the EU DEMO WCLL blanket concept, Fusion Eng. Des. 158 (2020) 111745 10.1016/j.fusengdes.2020.111745.

[15] X. Z. Jin, BB LOCA analysis for the reference design of the EU DEMO HCPB blanket concept, Fusion Eng. Des. 136 (B) (2018) 958-963 10.1016/j.fusengdes.2018.04.046.

[16] S. D'Amico, X. Z. Jin, F. Hernández, I. Moscato and G. Zhou, Preliminary thermal-hydraulic analysis of the EU-DEMO Helium-Cooled Pebble Bed fusion reactor by using the RELAP5-3D system code, Fusion Eng. Des. 162 (2021) 112111 10.1016/j.fusengdes.2020.112111.

[17] M.-Y. Ahn, S. Cho, D. H. Kim, E.-S. Lee, H.-S. Kim, J.-S. Suh, S. Yun and N. Z. Cho, Preliminary safety analysis of Korea Helium Cooled Solid Breeder Test Blanket Module, Fusion Eng. Des. 83 (10-12) (2008) 1753-1758 10.1016/j.fusengdes.2008.06.059.

[18] M. Nakamura, K. Tobita, Y. Someya, H. Utoh, Y. Sakamoto and W. Gulden, Thermohydraulic responses of a water-cooled tokamak fusion DEMO to loss-of-coolant accidents, Nucl. Fusion 55 (12) (2015) 123008 10.1088/0029-5515/55/12/123008.

[19] G. Caruso, CONSEN Version 4.0 - ' ''User's Guide, Installation and Input Files, SRS-ENEA-FUS, Frascati, Italy, February 1997.

[20] G. Caruso, F. Giannetti and M. T. Porfiri, Modeling of a confinement bypass accident with CONSEN, a fast-running code for safety analyses in fusion reactors, Fusion Eng. Des. 88 (2013) 3263–3271 10.1016/j.fusengdes.2013.10.004

[21] G. Caruso and M. T. Porfiri, Ice layer growth on a cryogenic surface in a fusion reactor during a loss of water event, Prog. Nucl. Energy 78 (2015) 173–181, 10.1016/j.pnucene.2014.09.015.

[22] M. T. Porfiri and P. Meloni, Post-test calculations with ISAS-ITER system for ICE experiments, in Proc. 19th IEEE/IPSS Symp. Fusion Eng. 19th SOFE (Cat. No.02CH37231), Atlantic City, NJ, USA (2002) 48-51 10.1109/FUSION.2002.1027639.

[23] G. Caruso, H. W. Bartels, M. Iseli, R. Meyder, S. Nordlinder, V. Pasler and M. T. Porfiri, Simulation of cryogenic He spills as basis for planning of experimental campaign in the EVITA facility, Nucl. Fusion 46 (2005) 51–56 10.1088/0029-5515/46/1/006.

[24] A. Froio, C. Bachmann, F. Cismondi, L. Savoldi and R. Zanino, Dynamic thermal-hydraulic modelling of the EU DEMO HCPB breeding blanket cooling loops, Prog. Nucl. Energy 93 (2016) 116-132 10.1016/j.pnucene.2016.08.007.

[25] A. Froio, F. Casella, F. Cismondi, A. Del Nevo, L. Savoldi and R. Zanino, Dynamic thermal-hydraulic modelling of the EU DEMO WCLL breeding blanket cooling loops, Fusion Eng. Des. 124 (2017) 887-891 10.1016/j.fusengdes.2017.01.062.

[26] A. Froio, F. Cismondi, L. Savoldi and R. Zanino, Thermal-Hydraulic Analysis of the EU DEMO Helium-Cooled Pebble Bed Breeding Blanket Using the GETTHEM Code, IEEE Trans. Plasma Sci. 45 (5) (2018)

1436-1445 10.1109/TPS.2018.2791678.
[27] A. Froio, A. Bertinetti, L. Savoldi, R. Zanino, S. Ciattaglia and F. Cismondi, Benchmark of the GETTHEM Vacuum Vessel Pressure Suppression System (VVPSS) model for a helium-cooled EU DEMO blanket, Proc. 27th European Safety and Reliability Conference, Portorož, Slovenia, 2017, in Safety and Reliability – Theory and Applications (2017) 59-66 10.1201/9781315210469-9.
[28] F. Casella and A. Leva, Modelling of Thermo-hydraulic Power Generation Processes Using Modelica, Math. Comput. Model. Dyn. Syst. 12 (1) (2006) 19-33 10.1080/13873950500071082.
[29] R. O. Gauntt et al., "MELCOR Computer Code Manuals vol. 1: Primer and Users"Guide Version 1.8.6, NUREG/CR-6119, vol. 1, Rev. 3, Sandia National Laboratory (2005).
[30] B. J. Merril, P. W. Humrickhouse and R. J. Moore, A recent version of MELCOR for fusion safety applications, Fusion Eng. Des. 85 (7-9) (2010) 1479-1483 10.1016/j.fusengdes.2010.04.017.
[31] B. J. Merrill, P. W. Humrickhouse and M. Shimada, Recent development and application of a new safety analysis code for fusion reactors, Fusion Eng. Des. 109-111 (A) (2016) 970-974.
[32] Idaho National Engineering and Environmental Laboratory, RELAP5-3D Code Manuals, INEEL-EXT-98-00834 (1999).
[33] X. J. Jin, B.-E. Ghidersa and A. F. Badea, HELOKA-HP thermal-hydraulic model validation and calibration, Fusion Eng. Des. 109–111 (B) (2016) 1242-1246 10.1016/j.fusengdes.2015.11.054.
[34] M. D'Onorio et al., Pressure suppression system influence on vacuum vessel thermal-hydraulics and on source term mobilization during a multiple first Wall – Blanket pipe break, Fusion Eng. Des. 164 (2021), 112224, 10.1016/j.fusengdes.2020.112224
[35] C. Gliss, KDI_6_TOKAMAK_COMPLEX_INTEGRATION_MODEL_02_15 (WCLL), CAD model, IDM ref. 2NNEGY